

Quarkonia Suppression in QGP Under Colour Screening Scenario at SPS, RHIC and LHC

P. K. Srivastava^a, M. Mishra^b and C. P. Singh^a

^a*Department of Physics, Banaras Hindu University, Varanasi - 221005, India*

^b*Birla Institute of Technology and Science, Pilani - 333031, India*

Abstract

We present a modified colour screening model for J/ψ suppression in the Quark-Gluon Plasma (QGP) using quasi-particle model (QPM) as equation of state (EOS). Other theoretical ingredients incorporated in the model are feed-down from higher resonances namely, χ_c , and ψ' , dilated formation time for quarkonia and viscous effects of the QGP medium. Assuming further that the QGP is expanding with Bjorken's hydrodynamical expansion, the present model is used to analyze the centrality dependence of the J/ψ suppression in mid-rapidity region and compare it with the data obtained from SPS, RHIC and LHC experiments. We find that the centrality dependence of the data for the survival probability at all energies is well reproduced by our model. We further compare our model predictions with the results obtained from the bag model EOS for QGP which has usually been used earlier in all such calculations and our results indicate that the present EOS yields a better result in comparison to the bag model.

PACS numbers : 12.38.Mh, 12.38.Gc, 25.75.Nq, 24.10.Pa

Keywords : Quark-Gluon Plasma; Colour Debye screening; Heavy-ion collisions; J/ψ suppression

1 Introduction

Ultra-relativistic collisions of heavy nuclei are believed to produce nuclear matter at extreme pressure and energy density. Quantum Chromodynamics (QCD) predicts that a deconfined state of partonic matter which is referred as the quark-gluon plasma (QGP), will be produced in such circumstances. One of the most striking signatures is the suppression of heavy quarkonia states such as the charmonia (J/ψ , ψ' , χ_c etc) in the deconfined state. Charmonia suppressions in heavy-ion collisions have been experimentally studied, first at the CERN Super Proton Synchrotron (SPS) by NA50 [2] and NA60 experiment [3] at $\sqrt{s_{NN}} = 17.3 - 19.3$ GeV and then at Relativistic Heavy Ion Collider (RHIC) by the PHENIX experiment at $\sqrt{s_{NN}} = 200, 39$ and 62.4 GeV [4], and now at Large Hadron Collider (LHC) by the CMS and ALICE experiments at $\sqrt{s_{NN}} = 2.76$ TeV [5, 6]. However, experimental results involve more puzzling features which defy explanations on the basis of colour-screening in the QGP alone. For example, we notice significantly less suppression at the mid-rapidity than at forward rapidity ($1.2 < |y| < 2.2$) while the medium in the central part of the collision is the most dense and intuitively one would expect an opposite behaviour. Another interesting experimental observation is similar J/ψ suppression at SPS and RHIC energies for same number of participants [4]. Many theoretical efforts have since been made which explore the effects of cold nuclear matter (CNM) as well as possible coalescence of originally uncorrelated c , \bar{c} quark pairs. However, the complete theoretical interpretation for J/ψ suppression is still lacking.

Many theoretical papers have analyzed the heavy-ion experimental data regarding nuclear modification factor for heavy quarkonia. For example, $Pb + Pb$ data at SPS explained by variety of models [7, 8, 9, 10, 11, 12, 13, 14] with or without deconfinement phase transition scenario. Yunpeng et al., [15] analyzed the J/ψ suppression data using a transport model calculation involving suppression as well as the regeneration of J/ψ due to coalescence of c and \bar{c} pair produced abundantly in the initial stage of collisions at RHIC and LHC energies. Zhen Qu et al., [16] used a similar approach to explain the forward rapidity data for J/ψ at RHIC energy. Sharma and Vitev [17] calculated the yields of quarkonia at RHIC and LHC as a function of transverse momentum based on heavy quark effective theory in which both colour singlet and colour octet contributions along with feed down effects from excited states were suitably incorporated. Their model provides good description of the LHC data for central as well as peripheral collisions. But none of the available models could provide a satisfactory and consistent explanation for the suppression at all energies simultaneously. We have recently modified the colour-screening model [18] of Chu and Matsui [19] by parametrizing pressure instead of energy density since pressure density becomes almost zero at the deconfinement phase transition point. We have further shown that the variation of survival probability of

J/ψ with respect to participant number obtained from this model compares well with the experimental data (CNM normalized) at RHIC [18]. In the present paper, we reinvestigate the colour-screening model by employing a more realistic thermodynamically-consistent quasi-particle prescription for the equation of state (EOS) of QGP medium. This highlights a major difference between our present approach and the model of Chu, Matsui [19] or Mishra et al [18] because bag model is still considered as a crude EOS for QGP. We have demonstrated earlier that various thermodynamical as well as transport quantities obtained from the present quasiparticle model (QPM) compare well with the most recent lattice results [20, 21]. In addition, we incorporate here viscous hydrodynamics in our formulation with a constraint that the ratio η/s varies very slowly [21] with the temperature in the QGP medium. This assumption helps us in taking η to be almost independent of the temperature. Feed down from higher resonances have also been incorporated in the model.

We use our formulation to explain the recent LHC experimental data on J/ψ suppression along with the RHIC and SPS data. We surprisingly find that J/ψ suppression at mid-rapidity is explained consistently by our model at SPS, RHIC and LHC energies in QGP picture alone. Further we compare results obtained from quasiparticle model (QPM) and the bag model EOS on J/ψ suppression and find that QPM EOS describes the data better in comparison to the bag model EOS for QGP and thus supports the utility of the present model in explaining J/ψ suppression.

2 Formulation

2.1 Cooling law

The main theme of the present formulation is essentially borrowed from our previous model [18] where we have used the colour screening idea of Chu and Matsui [19]. We have assumed that QGP medium formed during the collision, expands and cools according to the Bjorken's boost invariant longitudinal hydrodynamics in mid-rapidity region. Employing the conservation of energy-momentum tensor, the rate for the decrease of energy density ϵ [22] is given by

$$\frac{d\epsilon}{d\eta} = -\frac{\epsilon + p}{\tau} + \frac{4\eta}{3\tau^2}, \quad (1)$$

where η is the shear viscosity of the QGP medium, p is the pressure density and τ is the proper time. Using Eq.(1) and the thermodynamical identity $\epsilon = T \frac{dp}{dT} - p$, the cooling laws for energy density and pressure can

be separately derived as (see Appendix) :

$$\epsilon = c_1 + c_2 \tau^{-q} + \frac{4\eta}{3c_s^2} \frac{1}{\tau}, \quad (2)$$

$$p = -c_1 + c_2 \frac{c_s^2}{\tau^q} + \frac{4\eta}{3\tau} \left(\frac{q}{c_s^2 - 1} \right) + c_3 \tau^{-c_s^2}, \quad (3)$$

where c_1 , c_2 and c_3 are constants which can be determined by imposing the initial boundary conditions on energy density and pressure, $q = c_s^2 + 1$ with c_s as the speed of sound in the medium. The energy density and pressure are computed by employing quasiparticle model (QPM) EOS [20] for QGP. We take $\epsilon = \epsilon_0$ at $\tau = \tau_0$ (initial thermalization time) and $\epsilon = 0$ at $\tau = \tau'$; where τ' is the proper time. Consequently, the constants c_1 and c_2 are related as :

$$c_1 = -c_2 \tau'^{-q} - \frac{4\eta}{3c_s^2 \tau'} \quad (4)$$

, where $\tau' = \tau_0 A^{-\frac{3R}{R-1}}$, $A = T_0/T'$ and R is the Reynold's number for QGP. Further :

$$c_2 = \frac{\epsilon_0 - \frac{4\eta}{3c_s^2} \left(\frac{1}{\tau_0} - \frac{1}{\tau'} \right)}{\tau_0^{-q} - \tau'^{-q}}. \quad (5)$$

Using the other initial condition $p = p_0$ at $\tau = \tau_0$ gives the value of c_3 as follows :

$$c_3 = (p_0 + c_1) \tau_0^{c_s^2} - c_2 c_s^2 \tau_0^{-1} - \frac{4\eta}{3} \left(\frac{q}{c_s^2 - 1} \right) \tau_0^{(c_s^2 - 1)}. \quad (6)$$

2.2 Pressure Profile

Assuming that the pressure almost vanishes at the transition temperature $T = T_c$, we take a pressure profile function in the transverse plane with a transverse distance r as [18] :

$$p(t_i, r) = p(t_i, 0) h(r); \quad h(r) = \left(1 - \frac{r^2}{R_T^2} \right)^\beta \theta(R_T - r), \quad (7)$$

where the coefficient $p(t_i, 0)$ is yet to be determined, R_T denotes the radius of the cylindrical plasma and it is related to the transverse overlap area A_T as determined by Glauber model $R_T = \sqrt{\frac{A_T}{\pi}}$. The pressure is thus assumed to be maximum at the central axis but it vanishes at the edge R_T where hadronization occurs. The exponent β depends on the energy deposition mechanism and here we have taken $\beta = 1.0$ [18]; θ is the

unit step function. The factor $p(t_i, 0)$ is related to the average initial pressure $\langle p \rangle_i$ via

$$p(t_i, 0) = (1 + \beta) \langle p \rangle_i. \quad (8)$$

The above average pressure is determined by the centrality dependent initial average energy density $\langle \epsilon \rangle_i$ which is given by Bjorken's formula [23, 24] :

$$\langle \epsilon \rangle_i = \frac{1}{A_T \tau_i} \frac{dE_T}{dy}, \quad (9)$$

where dE_T/dy is the transverse energy deposited per unit rapidity. We use the experimental value of $dE_T/d\eta'$ where η' is the pseudorapidity and then multiply it by a corresponding jacobian factor [24, 25] in order to obtain dE_T/dy for a given number of participants (N_{part}) at a particular center-of-mass energy ($\sqrt{s_{NN}}$). Further at the initial proper time $\frac{\partial \langle p \rangle_i}{\partial \langle \epsilon \rangle_i} = \frac{\langle p \rangle_i}{\langle \epsilon \rangle_i} = c_s^2$ in QPM EOS [21] and thus $\langle p \rangle_i = c_s^2 \langle \epsilon \rangle_i$.

2.3 Constant Pressure Contour and Radius of Screening Region

Since the cooling law for pressure cannot be solved for τ analytically and therefore we use a trick to determine the radius of screening region. Writing the cooling law of pressure as follows :

$$p(\tau, r) = A + \frac{B}{\tau^q} + \frac{C}{\tau} + \frac{D}{\tau^{c_s^2}}, \quad (10)$$

where A , B , C and D are constants related to c_1 , c_2 and c_3 as : $A = -c_1$, $B = c_2 c_s^2$, $C = \frac{4\eta q}{3(c_s^2 - 1)}$ and $D = c_3$. Writing the above equation at the initial time $\tau = \tau_i$ and at screening time $\tau = \tau_s$ we get :

$$p(\tau_i, r) = A + \frac{B}{\tau_i^q} + \frac{C}{\tau_i} + \frac{D}{\tau_i^{c_s^2}} = p(\tau_i, 0)h(r), \quad (11)$$

and

$$p(\tau_s, r) = A + \frac{B}{\tau_s^q} + \frac{C}{\tau_s} + \frac{D}{\tau_s^{c_s^2}} = p_{QGP}. \quad (12)$$

Here p_{QGP} is the QGP pressure as determined by EOS in QPM [20, 21]. Solving Eqs. (11) and (12) numerically and equating the screening time τ_s to the dilated formation time of quarkonia $t_F (= \gamma \tau_F$ where $\gamma = E_T/M_\psi$ is the Lorentz factor associated with the transverse motion of the $c - \bar{c}$ pair and $M_\psi = 3.1$ GeV and τ_F is the proper time required for $c - \bar{c}$ for formation of J/ψ), we can find the radius of the screening region r_s . The screening region is defined as a region where temperature is more than the dissociation

temperature so that the quarkonia formation is unlikely inside that region [18]. Hence the pair will escape the screening region and form quarkonia if $|\vec{r}_\psi + \vec{v}t_F| \geq r_s$ where \vec{r}_ψ is the position vector at which the charm-quark pair created.

The above kinematic condition takes a simplified form by assuming that J/ψ is moving with transverse momentum p_T . Thus the above escape condition can be expressed as a trigonometric condition [18] :

$$\cos \phi \geq Y; \quad Y = \frac{(r_s^2 - r_\psi^2)m - \tau_F^2 p_T^2/m}{2r_\psi \tau_F p_T}, \quad (13)$$

where ϕ is the angle between the transverse momentum (p_T) and the position vector \vec{r}_ψ and $r_\psi = |\vec{r}_\psi|$ with $m = M_\psi$.

2.4 Survival Probability

Assuming the radial probability distribution for the production of $c\bar{c}$ pair in hard collisions at transverse distance r is

$$f(r) \propto \left(1 - \frac{r^2}{R_T^2}\right)^\alpha \theta(R_T - r). \quad (14)$$

Here we take $\alpha = 1/2$ in our calculation as used in Ref. [19]. Then, in the colour screening scenario, the survival probability for the quarkonia can easily be obtained as [18, 19] :

$$S'(p_T, N_{part}) = \frac{2(\alpha + 1)}{\pi R_T^2} \int_0^{R_T} dr r \phi_{max}(r) \left\{1 - \frac{r^2}{R_T^2}\right\}^\alpha, \quad (15)$$

where the maximum positive angle ϕ_{max} allowed by Eq. (13) becomes [18] :

$$\phi_{max}(r) = \begin{cases} \pi & \text{if } Y \leq -1 \\ \pi - \cos^{-1}|Y| & \text{if } 0 \geq Y \geq -1 \\ \cos^{-1}|Y| & \text{if } 0 \leq Y \leq 1 \\ 0 & \text{if } Y \geq 1 \end{cases}$$

Generally experimentalist measure the quantity namely, p_T integrated nuclear modification factor and therefore, the theoretical p_T integrated survival probability is of paramount importance to compare with the experimental results. It is defined as follows :

$$S'(N_{part}) = \frac{\int_{p_{Tmin}}^{p_{Tmax}} S'(p_T, N_{part}) dp_T}{\int_{p_{Tmin}}^{p_{Tmax}} dp_T}. \quad (16)$$

It has been found that only about 60% of the observed J/ψ come from hard collisions whereas 30% is from the decay of χ_c and 10% from the ψ' [18]. Therefore, the net survival probability of J/ψ in the presence of QGP medium is :

$$S_{J/\psi} = 0.60S'_{J/\psi} + 0.30S'_{\chi_c} + 0.10S'_{\psi'} \quad (17)$$

In our calculations we use $T_c = 0.17$ GeV in accord with the recent lattice QCD results, $\beta = 1.0$, and $\alpha = 0.5$ [18]. We take the masses as 3.1, 3.5 and 3.7 GeV of J/ψ , χ_c and ψ' , respectively [28]. Further we choose formation time τ_F as 0.89, 2.0 and 1.5 fm for J/ψ , χ_c and ψ' , respectively [28, 18]. We use these values of parameters at all $\sqrt{s_{NN}}$ in our calculations for survival probability.

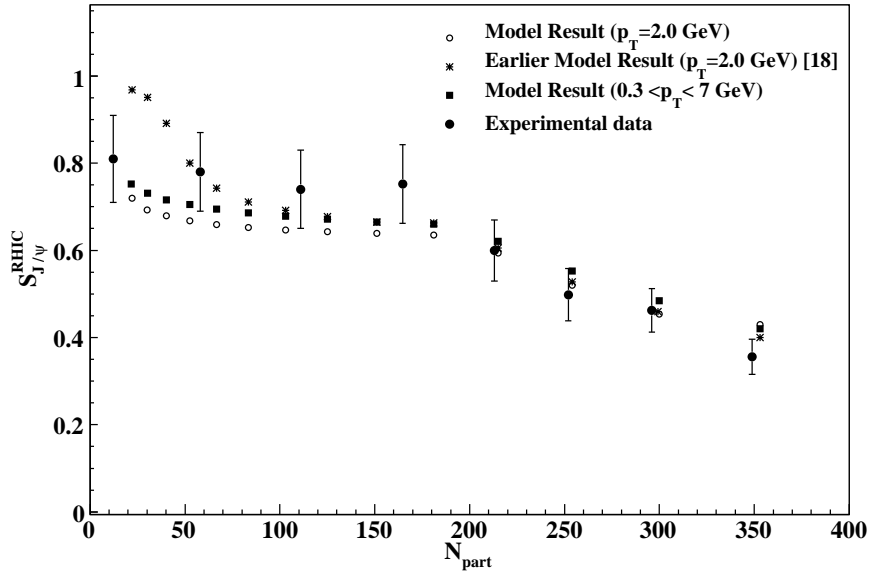


Figure 1: Variation of survival probability of J/ψ at RHIC energy ($S_{J/\psi}^{RHIC}$) with respect to N_{part} . Experimental data points are taken from Ref. [4].

3 Results and Discussions

Fig. 1 shows the variation of survival probability of J/ψ at RHIC energy (i.e. $\sqrt{s_{NN}} = 200$ GeV) with respect to N_{part} . Star symbols represent the results of Ref. [18] where a bag model EOS for QGP along

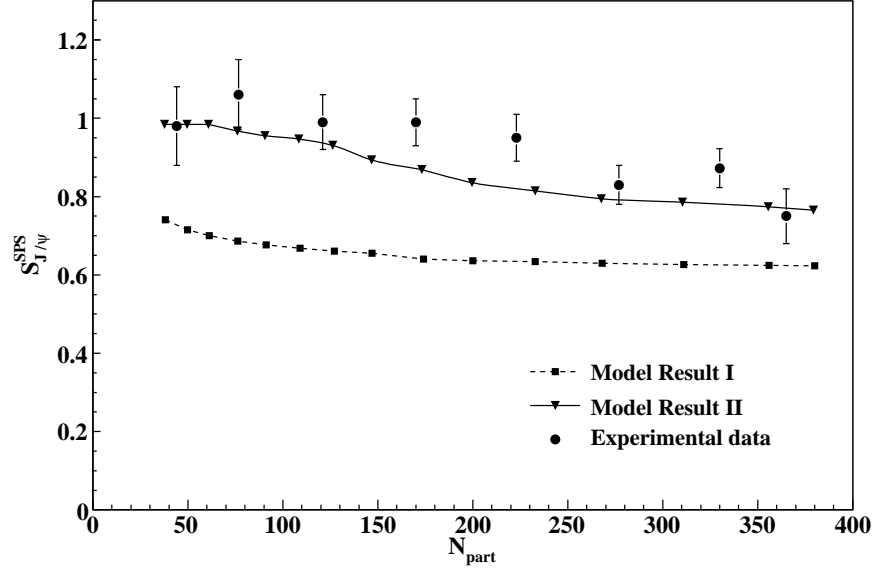


Figure 2: Variation of survival probability of J/ψ at SPS energy ($S_{j/\psi}^{SPS}$) with respect to N_{part} . Model I and Model II are our model with two different sets of dissociation temperatures (T_d) for J/ψ , χ_c and ψ' (details in text). Experimental data points are taken from Ref. [2].

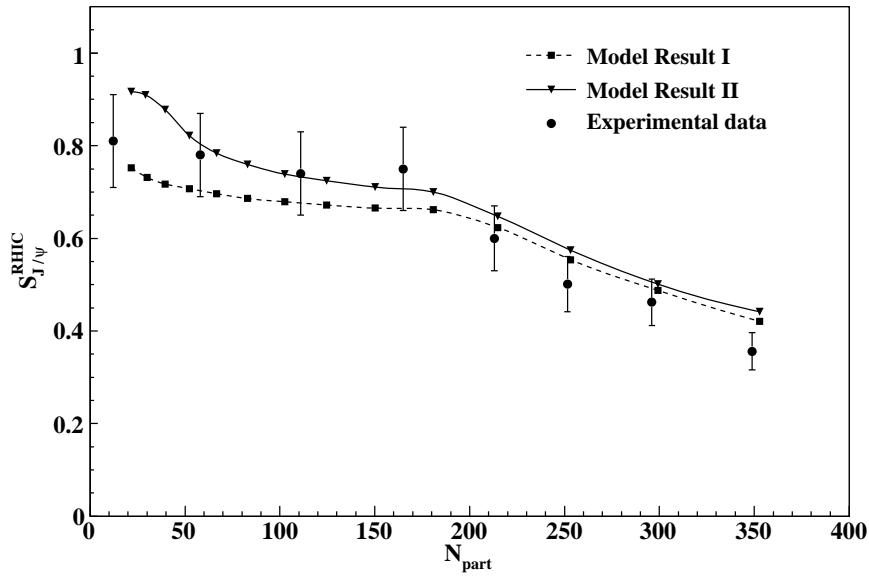


Figure 3: Variation of survival probability of J/ψ at RHIC energy ($S_{j/\psi}^{RHIC}$) with respect to N_{part} . Experimental data points are taken from Ref. [4].

with ideal hydrodynamics was used and $S_{j/\psi}^{RHIC}$ has been calculated at fixed $p_T = 2.0$ GeV with dissociation temperatures $T_d/T_c = 2.1, 1.16, 1.12$ for J/ψ , χ_c and ψ' , respectively [18]. Open circles are our model

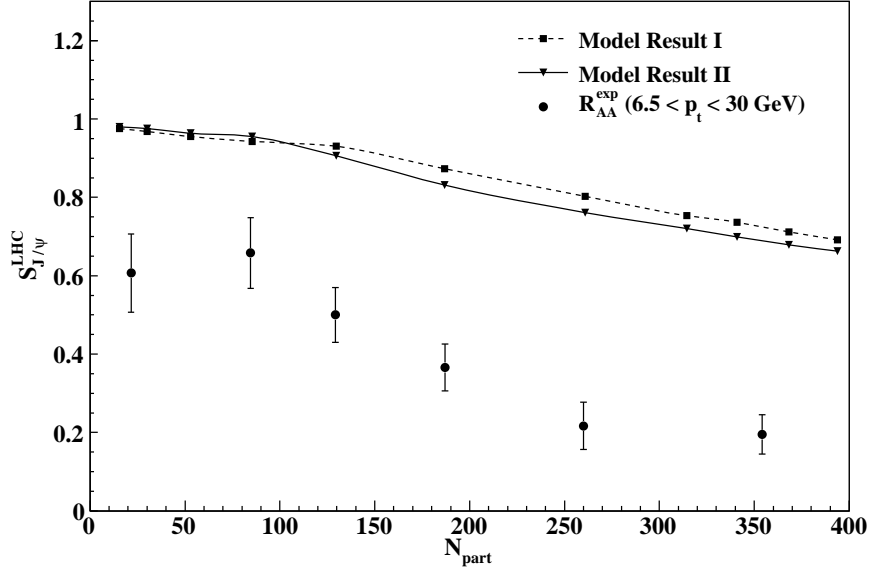


Figure 4: Variation of survival probability of J/ψ at LHC energy ($S_{j/\psi}^{LHC}$) with respect to N_{part} . Experimental data points are R_{AA}^{exp} for prompt J/ψ without any CNM normalization as taken from Ref. [5].

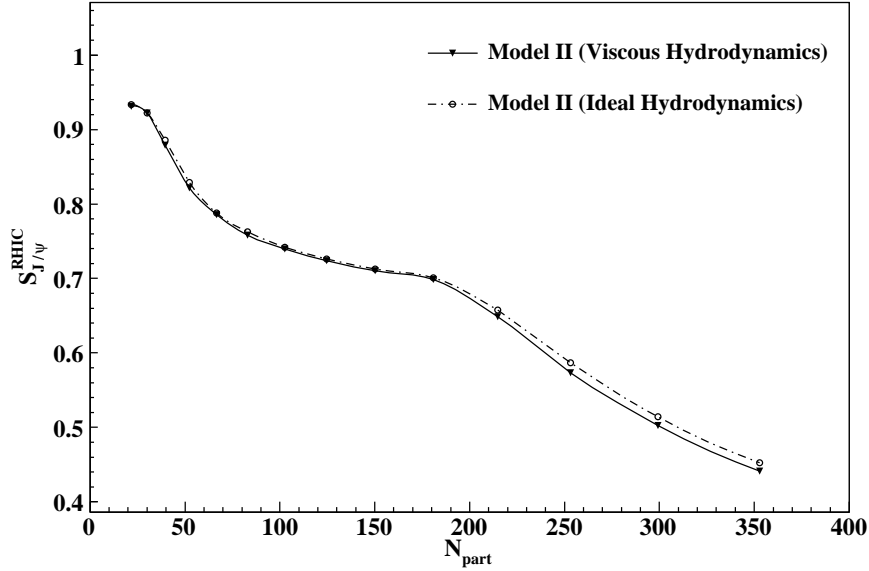


Figure 5: Variation of survival probability of J/ψ at RHIC energy ($S_{j/\psi}^{RHIC}$) with respect to N_{part} calculated within our model in viscous as well as in ideal hydrodynamics framework.

results where we have used QPM EOS along with viscous hydrodynamics and parameters have the same value [18]. The comparison shows that the results from our model provide a better description of the experimental data [4] (shown by solid points in Fig. 1) in comparison to the results obtained earlier [18].

Here experimental data have been normalized with CNM effect. We have also shown the p_T integrated variations of $S_{j/\psi}^{RHIC}$ with N_{part} obtained from our model, represented by solid inverse triangles, using the same values of dissociation temperature and observe that the agreement with the experimental data has improved.

Fig. 2 presents the variation of $S_{j/\psi}^{SPS}$ with N_{part} obtained from our model for two different sets of dissociation temperatures (labelled as Model I and Model II) and their comparison to the CNM normalized experimental data [4, 18]. Moreover, one should keep in mind that from here onwards, we use the same p_T range in all of our model calculations as used in related experimental data. In model I (shown by filled square), we have taken the dissociation temperatures $T_d/T_c = 2.1, 1.16$ and 1.12 for J/ψ , χ_c and ψ' [18] whereas model II (shown by solid triangle) gives the calculation for $T_d/T_c = 2.0, 1.5$ and 1.4 for J/ψ , χ_c and ψ' , respectively. In some recent lattice calculations [26, 27], after constant mode correction, there is no hint for suppression of χ_c and ψ' instantly after T_c as pointed out by earlier studies [28, 29, 30, 31, 32]. Due to above uncertainty regarding the dissociation temperatures of different quarkonia states, we wish to see the effect of T_d in explaining the data of RHIC and SPS experiments, simultaneously. We observe that the changes in T_d values produce more significant results in the peripheral collisions rather than in central collisions.

Fig. 3 demonstrates the variation of $S_{j/\psi}^{RHIC}$ with respect to N_{part} as obtained from model I and model II. Here we observe that except for extreme peripheral collisions, model II compares well with the experimental data (normalized with CNM effect) in comparison to model I for semi-central case and results from both models converge for central collisions. This again shows that a change in T_d values is more effective in peripheral collision rather than in the central collision. However, at RHIC energy the difference in the results of two models is insignificantly less in comparison to their results at SPS energy for all collision centrality. It may be due to the reason that when we increase the dissociation temperatures for χ_c and ψ' , the energy deposited in the collision at SPS energy is still not sufficient to melt all the χ_c s and ψ' s even in the central collisions and thus it provides a significant contribution to the survived J/ψ s. However, at RHIC, except for most peripheral collisions, the energy deposited in the collision zone becomes always sufficient to dissociate a significant fraction of χ_c s and ψ' s even if their dissociation temperature becomes higher as $1.5 T_c$ and $1.4 T_c$ from $1.16 T_c$ and $1.12 T_c$, respectively. Thus the contribution from χ_c and ψ' is less in the survival of J/ψ . Moreover, for most central collisions the contributions from χ_c and ψ' becomes negligible and the prediction of both the models overlap on each other.

Fig. 4 shows the variation of $S_{j/\psi}^{LHC}$ with respect to N_{part} obtained in our model I and II. Here we find that there is almost no difference in the survival probability calculated within model I and model II for all collision centrality. This means that the contribution to $S_{j/\psi}$ from χ_c and ψ' is almost negligible and the only

contribution to survival probability comes from J/ψ alone. We also present the recent experimental data of nuclear modification factor (R_{AA}) without any cold nuclear matter (CNM) effect correction for prompt J/ψ in mid-rapidity ($|y| < 2.4$) obtained by CMS collaboration [5]. The qualitative agreement of our prediction with the experimental data is reasonably good and quantitative agreement is expected only after normalizing the experimental data (nuclear modification factor) by the corresponding contribution from CNM effect (i.e., R_{AA}^{CNM}) at LHC energy.

In Fig. 5, we present our model results for $S_{j/\psi}^{RHIC}$ with N_{part} and also show a comparison with results obtained in our model when we put shear viscosity (η) equal to zero i.e., considering ideal hydrodynamic framework. We find that if we choose the value of $\eta/s = 1/4\pi$ (suggested as the lower limit for any fluid [33]) then the difference between ideal and viscous case vanishes. However, for larger values of η/s , the effect is expected to be sizable. We have also checked the difference between ideal and viscous case at SPS energy and find that the effect is further reduced in comparison to the results at the RHIC energy.

In summary, we have presented a modified colour-screening model for J/ψ suppression in QGP medium where quasi-particle model equation of state for QGP, feed down from higher resonance states (namely, χ_c , and ψ'), dilated formation time for quarkonia and viscous effect in the QGP medium have been properly taken into account. Furthermore, we assume that the QGP is expanding with Bjorken's boost invariant longitudinal expansion. The above model has been employed to analyze the centrality dependence of the J/ψ suppression data from SPS, RHIC and LHC experiments. We find that the centrality dependent survival probability is adequately reproduced by the current model in a consistent manner. We have also compared our present model results with the previous model results [18] where bag model EOS of QGP has been used. We notice that present model describes the experimental data better as compared to the old model [18]. Thus we conclude that our model provides a better explanation for the J/ψ suppression at SPS, RHIC and LHC experiments without any free parameter. Further extension of this work is underway to explain the complete rapidity dependence of the data in order to draw a firm conclusion regarding the overall level of suppression arising from QGP picture alone.

Acknowledgement

One of the author (M. Mishra) is grateful to the Department of Science and Technology (DST), New Delhi for financial assistance as FAST-Track Young Scientist project. P. K. Srivastava thanks the University Grant Commission, New Delhi for financial support.

References

- [1] T. Matsui and H. Satz, Phys. Lett. **178** (1986) 416.
- [2] M. C. Abreu et al., (NA50 Collaboration), Phys. Lett. B **477** (2000) 28; B. Alessandro et al., (NA50 Collaboration), Eur. Phys. J. C **39** (2005) 335.
- [3] R. Arnaldi et al. (NA60 Collaboration), Phys. Rev. Lett. **99**, (2007) 132302.
- [4] A. Adare et al., (PHENIX Collaboration), Phys. Rev. Lett. **98** (2007) 232301; arXiv:1208.2251v1[nucl-ex] (2012).
- [5] The CMS Collaboration, arXiv:1201.5069v1[nucl-ex] (2012).
- [6] The ALICE Collaboration, arXiv:1202.1383v1[hep-ex] (2012).
- [7] J. P. Blaizot and J.Y. Ollitrault, Phys. Rev. Lett. **77** (1996) 1703.
- [8] J. P. Blaizot, P. M. Dinh and J.Y. Ollitrault, Phys. Rev. Lett. **85** (2000) 4012.
- [9] A. Capella, E. G. Ferreira and A. B. Kaidalov, Phys. Rev. Lett. **85** (2000) 2080.
- [10] A. K. Chaudhuri, Phys.Rev. C **64** (2001) 054903 ; Phys.Lett. B **527** (2002) 80.
- [11] A. K. Chaudhuri, Phys. Rev. Lett. **88** (2002) 232302.
- [12] A. K. Chaudhuri, Phys. Rev.C **66** (2002) 021902.
- [13] A. K. Chaudhuri and Partha Pratim Bhaduri, arXiv:1202.3291[nucl-th] (2012), Phys. Rev. C (to be published).
- [14] L. Grandchamp, R. Rapp and G. E. Brown, Phys. Rev. Lett. **92** (2004) 212301.
- [15] Yunpeng Liu et al., J. Phys. G **37** (2010) 075110.
- [16] Zhen Qu et al., Nucl. Phys. A **830** (2009) 335c.
- [17] Rishi Sharma and Ivan Vitev, arXiv:1203.0329v1 [hep-ph] (2012).
- [18] M. Mishra, C. P. Singh, V. J. Menon and Ritesh Kumar Dubey, Phys. Lett. B **656** (2007) 45; M. Mishra, C. P. Singh and V. J. Menon, Proc. of QM, Indian. J. Physics **85** (2011) 849.
- [19] M.-C. Chu and T. Matsui, Phys. Rev. D **37** (1988) 1851.
- [20] P. K. Srivastava, S. K. Tiwari and C. P. Singh, Phys. Rev. D **82** (2010) 014023.
- [21] P. K. Srivastava and C. P. Singh, Phys. Rev. D **85** (2012) 114016.

- [22] D. A. Teaney, Int. J. Mod. Phys. E **21** (2009) 38.
- [23] J. D. Bjorken, Phys. Rev. D **27** (1983) 140.
- [24] S.S. Adler et al., (PHENIX Collaboration), Phys. Rev. C **71** (2005) 034908.
- [25] The CMS Collaboration, arXiv:1205.2488v1[nucl-ex] (2012).
- [26] H. Lida et al., Prog. of Theor. Phys. Suppl. **174**, (2008) 238.
- [27] T. Umeda, PoSLAT **2007** (2007) 233.
- [28] H. Satz, J. Phys. G **32** (2006) R 25.
- [29] S. Datta, F. Karsch, P. Petreczky and I. Wetzorke, Phys. Rev. D **69** (2004) 094507.
- [30] G. Aarts, C. Allton, M. B. Oktay, M. Peardon and J. I. Skullerud, Phys. Rev. D **76** (2007) 094513.
- [31] A. Jakovac, P. Petreczky, K. Petrov and A. Velytsky, Phys. Rev. D **75** (2007) 014506.
- [32] M. B. Oktay et al., PoSLAT **2007** (2007) 227.
- [33] P. Kovtun, D. Son, and A. Starinets, Phys. Rev. Lett. **94** (2005) 111601.

Appendix

(1+1)-Dimension Cooling Law for Temperature

To determine the explicit proper time (τ) dependence of temperature (T), we first start with the entropy equation for (1+1)-dimension expansion in (3+1)-dimension space given as follows [PRD 41, 2903 (1990)]:

$$\left[\frac{\partial(s\tau)}{\partial\tau} \right] \frac{1}{\tau} = \frac{s}{R\tau}, \quad (18)$$

where s is the entropy density of the system and R is the Reynold's number defined as follows for this system having shear and bulk viscosity as η and ζ , respectively:

$$\begin{aligned} R^{-1} &= \frac{4/3 \eta + \zeta}{T s \tau} \\ &= \frac{4}{3} \frac{\eta}{T s \tau} \quad (if \zeta = 0). \end{aligned} \quad (19)$$

After differentiating Eq. (18) with respect to τ we get :

$$3\tau \frac{\partial T}{\partial \tau} = T \left(1 - \frac{1}{R} \right). \quad (20)$$

We can rewrite the above Eq. (20) as follows :

$$3 \frac{\partial T}{T} = \left(1 - \frac{1}{R} \right) \frac{\partial \tau}{\tau}. \quad (21)$$

After integrating both side of the Eq.(21), we get :

$$3 \ln T = \left(1 - \frac{1}{R} \right) \ln \tau + \ln C, \quad (22)$$

or,

$$T^3 = \left(C \tau^{(1-1/R)} \right). \quad (23)$$

Using the boundary condition : $T = T_0$ at $\tau = \tau_0$ in Eq. (23), we get the value of C as :

$$C = \frac{T_0^3}{\tau_0^{(1-1/R)}}. \quad (24)$$

Finally, using the above value of constant C in Eq. (23), we get the 1+1 cooling law for temperature as below :

$$\left(\frac{T}{T_0}\right)^3 = \left(\frac{\tau}{\tau_0}\right)^{(1-1/R)}. \quad (25)$$

(1+1)-Dimension Cooling Law for Energy Density

The rate equation for energy density in Bjorken longitudinal expansion scenario for viscous case is as follows :

$$\frac{\partial \epsilon}{\partial \tau} = -\frac{\epsilon + p}{\tau} + \frac{4\eta}{3\tau^2}, \quad (26)$$

and the thermodynamical relation between ϵ and p in quasiparticle model (QPM) can be given as below [19]:

$$\epsilon = T \frac{\partial p}{\partial T} - p. \quad (27)$$

Differentiating (27) w.r.t. τ , we get the following relation :

$$\frac{\partial \epsilon}{\partial \tau} = \frac{\partial T}{\partial \tau} \frac{\partial p}{\partial T} + T \frac{\partial^2 p}{\partial T^2} - \frac{\partial p}{\partial \tau} \quad (28)$$

After equating Eq. (28) with Eq. (26) and putting $\epsilon + p = T \frac{\partial p}{\partial T}$, we got the following equation :

$$-\frac{T}{\tau} \frac{\partial p}{\partial T} + \frac{4\eta}{3\tau^2} = (T \frac{\partial^2 p}{\partial T^2} + \frac{\partial p}{\partial T}) \frac{\partial T}{\partial \tau} - \frac{\partial p}{\partial \tau} \quad (29)$$

Writing Eq. (26) as :

$$\frac{\partial \epsilon}{\partial \tau} = -\frac{T}{\tau} \frac{\partial p}{\partial T} + \frac{4\eta}{3\tau^2} \quad (30)$$

Differentiating the above Eq. (30) two times and eliminated $(T \frac{\partial^2 p}{\partial T^2} + \frac{\partial p}{\partial T}) \frac{\partial T}{\partial \tau}$ with the help of Eq. (29), we get

$$\tau \frac{\partial^2 \epsilon}{\partial \tau^2} + 2 \frac{\partial \epsilon}{\partial \tau} + \frac{4\eta}{3\tau^2} + \frac{\partial p}{\partial \tau} = 0. \quad (31)$$

We can rewrite Eq. (31) as :

$$\tau^2 \frac{\partial^2 \epsilon}{\partial \tau^2} + (2 + c_s^2) \tau \frac{\partial \epsilon}{\partial \tau} = -\frac{4\eta}{3\tau}. \quad (32)$$

Solution of Eq. (32) is given by :

$$\epsilon = c_1 + c_2 \tau^{-(c_s^2+1)} + \frac{4\eta}{3c_s^2} \frac{1}{\tau} \quad (33)$$

(1+1)-Dimension Cooling Law for Pressure

Again start from energy density rate equation :

$$\frac{\partial \epsilon}{\partial \tau} = -\frac{\epsilon + p}{\tau} + \frac{4\eta}{3\tau^2}. \quad (34)$$

It can be further written as :

$$\frac{\partial \epsilon}{\partial p} \frac{\partial p}{\partial \tau} = -\frac{\epsilon}{\tau} - \frac{p}{\tau} + \frac{4\eta}{3\tau^2}. \quad (35)$$

Since in QPM EOS, we know that $\partial p / \partial \epsilon = c_s^2$, thus the above Eq. (34) can be rewritten as :

$$\frac{\partial p}{\partial \tau} + c_s^2 \frac{p}{\tau} = -c_s^2 \frac{\epsilon}{\tau} + c_s^2 \frac{4\eta}{3\tau^2}. \quad (36)$$

Now, using the value of ϵ from Eq. (32), we get the final differential equation for the cooling law of pressure is as follows :

$$\frac{\partial p}{\partial \tau} + c_s^2 \frac{p}{\tau} + \frac{c_s^2}{\tau} c_1 + \frac{c_s^2}{\tau} c_2 \tau^{-(c_s^2+1)} - \frac{4\eta}{3\tau^2} (1 + c_s^2). \quad (37)$$

To solve this above partial differential equation, we need to determine its integrating factor (I.F.) which comes out to be $\tau^{c_s^2}$. Further we can write the solution of Eq. (36), by using this I.F. as follows :

$$p \tau^{c_s^2} = - \int \left(\frac{c_s^2}{\tau} c_1 + \frac{c_s^2}{\tau} c_2 \tau^{-(c_s^2+1)} - \frac{4\eta}{3\tau^2} (1 + c_s^2) \right) \tau^{c_s^2} d\tau \quad (38)$$

$$p = -c_1 + c_2 \frac{c_s^2}{\tau(c_s^2+1)} + \frac{4\eta}{3\tau} \left(\frac{c_s^2+1}{c_s^2-1} \right) + c_3 \tau^{-c_s^2}. \quad (39)$$

Or,

$$p = -c_1 + c_2 \frac{c_s^2}{\tau^q} + \frac{4\eta}{3\tau} \left(\frac{q}{c_s^2-1} \right) + c_3 \tau^{-c_s^2}, \quad (if \quad q = c_s^2 + 1) \quad (40)$$

Evaluation of constants c1, c2 and c3

Using the first boundary condition $\epsilon = \epsilon_0$ at $\tau = \tau_0$ in Eq. (33), we get the first constraint relation as follows :

$$\epsilon_0 = c_1 + c_2 \tau_0^{-q} + \frac{4\eta}{3c_s^2} \frac{1}{\tau_0} \quad (41)$$

Similarly, using second boundary condition $\epsilon = 0$ at $\tau = \tau'$ (corresponds to temperature $T' = 160 \text{ MeV}$) in Eq. (33), we get the second constraint relation as follows :

$$0 = c_1 + c_2 \left[\tau_0 \left(\frac{T'}{T_0} \right)^{3/(1-R^{-1})} \right]^{-(c_s^2+1)} + \frac{4\eta}{3c_s^2} \frac{1}{\tau_0} \left(\frac{T_0}{T'} \right)^{3/(1-R^{-1})}. \quad (42)$$

Subtracting Eq. (42) from Eq. (41), the expression to calculate c_2 is given below :

$$c_2 = \frac{\epsilon_0 - \frac{4\eta}{3c_s^2} \left(\frac{1}{\tau_0} - \frac{1}{\tau'} \right)}{\tau_0^{-q} - \tau'^{-q}}, \quad (43)$$

where τ' is calculated from Eq. (25). Consequently c_1 can be calculated from the following relation :

$$c_1 = -c_2 \tau'^{-q} - \frac{4\eta}{3c_s^2 \tau'}. \quad (44)$$

Finally, using initial condition $p = p_0$ at $\tau = \tau_0$ in Eq. (40), we can get the following expression to calculate c_3 as :

$$c_3 = (p_0 + c_1) \tau_0^{c_s^2} - c_2 c_s^2 \tau_0^{-1} - \frac{4\eta}{3} \left(\frac{q}{c_s^2 - 1} \right) \tau_0^{(c_s^2-1)}. \quad (45)$$